

# A Bayesian Approach to Modal Acoustic Emission Source Location

## *Un enfoque bayesiano para la ubicación de la fuente de emisión acústica modal*

Boris A. Zárate\*

<sup>a\*</sup> PhD, Researcher, Grupo de Investigación en Ingeniería Sísmica, Eólica, Geotécnica y Estructural (G-7). Escuela de Ingeniería Civil y Geomática, Boris.Zarate@nexteraenergy.com, 0000 0001 8141 0527, Universidad del Valle. Cali, Colombia

**Forma de citar:** Boris A. Zárate. A Bayesian Approach to Modal Acoustic Emission Source Location. *Eco Matemático*, 10 (1), 6-18

Recibido: 6 agosto 2018

Aceptado: 2 noviembre 2018

### Palabras clave

Inferencia  
Bayesiana, Emisión  
Acústica Modal,  
Localización del  
evento

**Resumen:** La Emisión Acústica Modal (MAE) es una rama de la Emisión Acústica (AE) con capacidades probadas para el Monitoreo de la Salud Estructural (SHM) de estructuras similares a placas. La MAE se diferencia de la AE en que la MAE utiliza la comprensión de la propagación de la onda para caracterizar y localizar la fuente. El análisis de la forma de onda incluye el uso de técnicas de frecuencia de tiempo para determinar el Tiempo de Llegada (TOA) de los diferentes modos. En este documento se propone el uso de la inferencia bayesiana para cuantificar la incertidumbre en la localización de la fuente para dos técnicas diferentes de localización del MAE. La primera técnica utiliza sólo el TOA del modo extensional (simétrico), mientras que la segunda técnica utiliza el TOA tanto del modo extensional como del modo flexural (antisimétrico). La ondícula de Morlet se utiliza para determinar el escalograma de la forma de onda. El escalograma se reasigna y se utiliza la Cadena de Markov Monte Carlo (MCMC) para muestrear la distribución posterior construida a través de la inferencia bayesiana. Los resultados se presentan a partir de la localización de las roturas de la mina del lápiz (PLBs) en una placa de aluminio de 1/8in de espesor y 36in por 36in. Los resultados muestran que el uso del TOA de sólo el modo simétrico conduce a un nivel más bajo de incertidumbre en comparación con el uso de ambos modos de extensión y flexión, debido a la dificultad de evaluar el tiempo de llegada del modo de flexión.

### Keywords

Bayesian Inference,  
Modal Acoustic  
Emission,

**Abstract:** Modal Acoustic Emission (MAE) is a branch of Acoustic Emission (AE) with proven capabilities for Structural Health Monitoring (SHM) of plate-like structures. MAE differs from AE in that MAE uses the understanding of the wave propagation to characterize and locate the source. The analysis of the waveform includes the use of time frequency techniques to determine the Time Of Arrival (TOA) of the different modes. This paper proposes the use of Bayesian inference to quantify the uncertainty in

\*Autor para correspondencia [boriszar@gmail.com](mailto:boriszar@gmail.com)

<http://dx.doi.org/10.1016/j.eq/>

2590-9215© 2017 Universidad Francisco de Paula Santander. Este es un artículo bajo la licencia CCBYNCND

## Event Location

the source location for two different MAE location techniques. The first technique uses only the TOA of the extensional (symmetric) mode, while the second technique uses the TOA of both extensional and flexural (antisymmetric) modes. The Morlet wavelet is used to determine the scalogram of the waveform. The scalogram is reassigned and Markov Chain Monte Carlo (MCMC) is used to sample the posterior distribution built through Bayesian inference. Results are presented from location of Pencil Lead Breaks (PLBs) in an aluminum plate of 1/8in of thickness and 36in by 36in. Results show that using the TOA of only the symmetric mode leads to a lower level of uncertainty compared to using both extensional and flexural modes, because of the difficulty in assessing the time of arrival of the flexural mode.

## Introduction

Acoustic Emission (AE) is a Non-Destructive Testing (NDT) method that allows in situ monitoring of structures and has been successfully used in different Structural Health Monitoring (SHM) applications (Cuadra and Vanniamparambil et al 2015, Zárate and Caicedo et al 2012, Ozevin and Hardin 2012). AE uses the sound waves that propagate through the material in the frequency range from 100kHz to 1MHz. These sound waves are typically Rayleigh and Lamb waves and are generated by events in the material such as the formation or growth of a crack (Scruby 1987). The transient waves are converted into a voltage by AE sensors, and digitalized by the data acquisition system. The waveforms obtained are processed and different features such as TOA, waveform maximum amplitude, duration, absolute energy, and rise time are calculated (Nair and Cai 2010). An amplitude threshold is used to trigger the processing of an individual AE waveform known as hit and determine the TOA. AE has become popular within the NDT community because (Shigeishi, Colombo et al. 2001) it allows: i) in-service structural health monitoring that can be adopted in an online monitoring fashion; ii) adaptability to any geometry or structural element; iii) simple and economic installations; and iv) wireless communication for collection and processing of data remotely (Godinez-Azcuaga, Inman et al. 2011).

Modal Acoustic Emission (MAE) is a branch of AE that considers the understanding of the wave propagating through the medium to characterize

and localize the source of the AE. The wave propagation modes are considered in to the analysis by identifying the arrival time of the different modes within the waveform. The sensors used in MAE are generally wide band with broader range, up to the lower ultrasonic. MAE analyses the waveforms captured by the sensors using time-frequency techniques such as Short Fourier Transforms, Wavelets or the Wigner-Vile Distribution. MAE has been successfully used for assessment of structures including pressure vessels, aircrafts (Geng 2006), pipe lines (Jiao and He et al 2004) and composites (Martine-Jequier and Gallego 2015). MAE has been adopted by the NDT community and included in different codes such as the ISO-19016 and NB-10-601. MAE has been very successful because its ability to characterize the source and locate AE events considering different wave propagation modes. Given that a single waveform captured by a sensor contains information of different TOA modes, the distance from the source to the sensor can be calculated. On the contrary location algorithms in AE are based on threshold crossing, which is associated to a specific mode and speed based on previous wave velocities tests. Still, the fact that the wave velocity is dependent on the mode and frequency of waves propagating in plates is one of the main sources of uncertainty in AE source location.

Traditional source location algorithms in AE and MAE do not account for uncertainties. The next generation of AE and MAE source location algorithms should consider different sources of uncertainty and estimate the uncertainty of the calculated location. Therefore, the location algorithm

should locate the event to a region of high probability rather than to a single point. The size of the region of high probability reflects on the level of uncertainties in the experimental data and parameters involved in the location.

Algorithms that account for uncertainties in AE source location have been developed but are not common in the literature. For instance, Niri and Salamone (2012) developed a probabilistic framework for AE source location in plate-like structures. The framework considers the uncertainty in the TOA of the wave and the wave velocity to point to a region of high probability where the event could be located. The methodology identifies the TOA and its uncertainty using the Continuous Wavelet Transform (CWT) with the complex Morlet wavelet. The framework assumes the probability distribution of the source location is a Gaussian distribution which mean and variance are estimated using the Extended Kalman Filter (EKF). The methodology was validated experimentally with Pencil Lead Breaks (PLBs) on an aluminum plate of 60cm by 60cm. Results show that region of high probability created by the framework encloses the location of the actual PLBs locations. Schumacher, Straub et al (2012) proposed a framework for Bayesian AE source location to estimate the region of high probability where the event might be located. Uncertainties from variability in the wave propagation and TOA of the wave are considered in the Bayesian framework. The Bayesian framework was validated using PLBs on a section of a bridge column of reinforced concrete of 61cm by 61cm by 183cm. Results show that the Bayesian framework estimates the region that encloses the actual PLBs location. Yan and Tang (2013) proposed a Bayesian framework for the location of AE sources in plate-like structures. The Bayesian framework accounts for uncertainties in the TOA of the wave and the wave velocity. The uncertainty in the wave TOA is estimated using CWT with the Complex Morlet wavelet. The framework was validated performing PLBs in a stiffed aluminum plate 600mm by 400mm and

2mm thick. Results show that the region of high probability generated by the Bayesian framework encloses the actual location of the PLBs. Zárate and Pollock et al (2015) proposed a Bayesian AE source location framework for AE events on the shell of a water-filled tank. The model considers the wave travelling through the liquid as well as the shell and accounts for different sources of uncertainty, such as the TOA, and the wave speed in the liquid and the shell. The Bayesian framework was validated using PLBs performed on the shell of a 29000-gallons rail road tank car. Results from the Bayesian framework show regions of high probability that encloses the actual location of the PLBs.

This paper proposes the use of Bayesian inference to quantify the uncertainty in the location calculated by two MAE location techniques. The first location technique is based only on the TOA of the extensional mode (S<sub>0</sub>), while the second technique uses both the extensional (S<sub>0</sub>) and the flexural (A<sub>0</sub>) modes. The reassigned scalogram calculated with the Morlet wavelet is used to determine the TOA of the different modes. Markov Chain Monte Carlo (MCMC) is used to sample the posterior distribution. Results are presented from location of Pencil Lead Breaks (PLBs) in an aluminum plate of 1/8in of thickness and 36in by 36in.

### Wave propagation in plates

Waves propagating in thin plates are known as Lamb waves and propagate in two types of modes: extensional (symmetric) and flexural (asymmetric). Lamb waves are dispersive, that is their velocity is a function of the mode, frequency and thickness (more about waves propagating in plates can be found at Rose 1999, Giugitui 2008). This characteristic of the waves propagating in thin plates is the most common source of error in AE source location, because the difficulty on determining the correct speed for the waveform captured by the sensor.

AE Sources located at a plate generate Lamb waves that propagate through the shell in two types of modes: symmetric and asymmetric. In an unbounded plate the asymmetric and symmetric modes can be described as (Giugitiu 2008)

$$\frac{\tan(hq)}{\tan(hp)} = \frac{4pq\xi^2}{(\xi^2 - q^2)^2} \quad (1)$$

$$\frac{\tan(hq)}{\tan(hp)} = -\frac{(\xi^2 - q^2)^2}{4pq\xi^2} \quad (2)$$

where  $\xi$  is the wave number and  $h$  is the half plate thickness. The terms  $p$  and  $q$  can be expressed in terms of the angular frequency  $\omega$ , the symmetric mode velocity  $c_e$ , and the asymmetric mode velocity  $c_f$  as

$$q = \sqrt{\frac{\omega^2}{c_e^2} - \xi^2} \quad (3)$$

$$p = \sqrt{\frac{\omega^2}{c_f^2} - \xi^2} \quad (4)$$

Notice from Eq. (1) to (4) that the wave number  $\xi$  is dependent of the angular frequency  $\omega$ . This characteristic of the Lamb waves is known as velocity dispersion and implies that the wave velocity is a function of the frequency and mode.

AE sensors capture packages of Lamb waves which velocities are known as group velocity and are dispersive as well. Group velocity can be calculated from the wave velocity  $c$  as (Giugitiu 2008)

$$c_g = c - \lambda \frac{\partial c}{\partial \lambda} \quad (5)$$

where  $\lambda$  is the wave length. This group velocity should match the energy content of the scalograms presented in the following section and will allow for the determination of the time of arrival of the first symmetric (S0) and first asymmetric (A0) modes.

### Time frequency analysis of the waveforms

The determination of the TOA of the wave is challenging and the most common cause of error in AE source location because of the dispersive nature of the waves that propagate in thin plates. It can be observed that given enough distance from the source to the sensors different packages of the wave arrive at different times. Hence, different waveform features typically used in AE analysis such as amplitude and average frequency are affected by the dispersion phenomenon (Aggelis and Matikas 2012). Early research efforts used the Fast Fourier Transforms (FFT) on each individual package of waves in order to determine the frequency content of the specific group of waves arriving (Alleyne and Cawley 1991, Eisenhart, Jacobs et al. 1999). This methodology was followed by the use of different time frequency analysis techniques on the complete captured waveform, which allowed to determine the TOA of the different frequency components. The Continuous Wavelet Transform (CWT) was chosen in here to determine the wave TOA.

The CWT is chosen in this study because CWT increases the time-frequency resolution by using narrow windows at high frequencies and wide windows at low frequencies, while all other time frequency techniques use a constant scale window. The consequence is that for the CWT uncertainty in time is a function of the frequency assigning low uncertainties in time to low frequencies. This property of the wavelets is known as multi-resolution and the scalable window is known as mother wa-

velet. The theoretical background for the Wavelet Transform was first proposed by Grossmann and Morlet (1984) and is expressed as

$$WT_x^{(\psi)}(s, \tau) = \frac{1}{\sqrt{s}} \int_{-\infty}^{\infty} f(t) \Psi^* \left( \frac{t - \tau}{s} \right) dt \quad (6)$$

where  $f(t)$  is the time domain signal,  $s$  is a positive scale,  $\tau$  is a translation parameter that localizes the wavelet in time, and  $\Psi^*(t)$  is the complex conjugate of the mother wavelet. The proposed framework uses the Morlet wavelet which was first proposed by Goupillaud and Grossman et al 1984 and is defined as

$$\Psi(t) = \pi^{-1/4} e^{i w_0 t} e^{-t^2/2} \quad (7)$$

where  $w_0$  is the dimensionless frequency.

The time-frequency resolution can be refined using the reassignment method proposed by Auger and Flandrin (1995) where the reassigned frequency and time can be calculated as

$$\hat{t}_x(t, s) = t + s \Re \left\{ WT_x^{(>t\psi)}(t, s) / WT_x^{(\psi)}(t, s) \right\} \quad (8)$$

$$\hat{s}_x(t, s) = \frac{-s w_0}{\Im \left\{ WT_x^{(>d\psi/dt)}(t, s) / WT_x^{(\psi)}(t, s) \right\}} \quad (9)$$

where  $\Re$  and  $\Im$  are the real and imaginary components of the complex number. As shown by Niethammer and Jacobs et al (2000) the reassigned scalogram can be used in here for developing the dispersion curves of the S0 and A0 modes propagating in a plate. The TOA of the S0 and A0 modes is obtained by superposing the theoretical mode and the scalograms, then the TOA data is used to feed the Bayesian framework for source location described in the following section.

## Bayesian framework for source location

Uncertainty in the context of numerical models represents the lack of knowledge that results when a prediction is performed. It arises from the fact that numerical models are idealizations of the natural phenomena and depend on variables that are unknown (Jaynes 2003). There are two types of uncertainty: epistemic and random. Epistemic uncertainty can be reduced with a better knowledge of the system, while random uncertainty cannot be reduced. The framework for source location proposed in this paper models uncertainty by using probability. Probability theory requires expressing knowledge and beliefs in probabilistic terms which can be challenging. Nevertheless, probability theory is theoretically adequate to model any type of uncertainty, especially when there is lack or imprecise field observations (O'Hagan and Oakley (2004)). In this context probability is used in numerical models as measure of the degree of knowledge or belief of some parameters used in the model and not as the traditional occurrence frequency of an event (Beck and Katafygiotis 1998, Kennedy and O'Hagan 2001). For instance, in the context of AE source location the unknown parameters are represented by the variables that define the numerical model of the wave propagation phenomena such as velocities of the different wave modes, or the TOA of these modes.

In the case of the first MAE methodology that uses only information from the extensional mode, consider that the calculated TOA with respect to the first hit of a subsequent  $i$ -th hit that belong to the same event is given by

$$\Delta t(\Theta)_i^{num} = \frac{d_{0-1}(x_1, y_1, x_0, y_0) - d_{0-i}(x_i, y_i, x_0, y_0)}{v_e} \quad (10)$$

where  $\Theta$  represents some unknown parameters;  $v_e$  is the wave velocity of the extensional mode;  $d_{(0-1)}$  and  $d_{(0-i)}$  are the distances traveled by the wave from the source to the sensors detecting

the first hit and the subsequent  $i$ -th hit;  $x_1$  and  $y_1$  represent the location of the sensor detecting the first hit;  $x_i$  and  $y_i$  represent the location of the subsequent  $i$ -th hit, and  $x_0$  and  $y_0$  represent the location of the source. Therefore, the difference between the measured TOA of the  $i$ -th hit with respect to the first hit  $\Delta t_i^{data}$  and the calculated TOA of the same  $i$ -th hit with respect to the first hit  $\Delta t_i^{num}$  can be calculated as

$$\delta_i = \Delta t_i^{data} - \Delta t(\Theta)_i^{num} \quad (11)$$

Notice that the term  $\delta_i$  results from the combination of both modeling and measurement errors and represents the difference between the outcome of the chosen numerical model  $M$ , which depends on some modeling parameters and the experimental data  $D$ . Marginalizing and assuming the term  $\delta_i$  is a realization of a zero-mean Gaussian distribution, it can be found that

$$p(D|\Theta, \mathcal{M}) \propto \prod_{i=1}^n \exp\left(-\frac{1}{2}\left(\frac{\Delta t_i^{data} - \Delta t(\Theta)_i^{num}}{\sigma_{\Delta t_{1-i}}}\right)^2\right) \quad (12)$$

where  $\sigma_{\Delta t_{1-i}}$  is the square root of the variance of the arrival time of the subsequent  $i$ -th hit with respect to the first hit found with the CWT and  $n$  is the number of hits obtained after the first hit. Notice that in Eq. (12) a minimum of three hits is required for planar location.

In the case of the second MAE location methodology that considers both extensional and flexural modes for a sensor that captures a waveform the distance from the sensor to the source can be written as

$$d_{0-i}^{data} = \frac{toa_f - toa_e}{\frac{1}{v_f} - \frac{1}{v_e}} \quad (13)$$

where  $d_{0-i}^{data}$  is the theoretical distance from the  $i$ -th sensor to the source;  $toa_f$  is the TOA of the flexural mode;  $toa_e$  is the TOA of the extensional mode and  $v_f$  is the velocity of the flexural mode. Therefore, the error function  $\delta_i$  can be calculated as

$$\delta_i = d_{0-i}^{data} - d_{0-i}(\Theta)^{num} \quad (14)$$

where  $d_{0-i}(\Theta)^{num}$  is the distance from the  $i$ -th sensor to the source as a function of the parameters  $\Theta$ . Assuming a zero-mean Gaussian distribution can be found that

$$p(D|\Theta, \mathcal{M}) \propto \prod_{i=1}^n \exp\left(-\frac{1}{2}\left(\frac{d_{0-i}^{data} - d_{0-i}(\Theta)^{num}}{\sigma_{d_{0-i}}}\right)^2\right) \quad (15)$$

where  $\sigma_{d_{0-i}}$  is the square root of the variance of the distance between the  $i$ -th sensor and the source. Notice that a minimum of 2 sensors is required to locate the source in the plane.

The parameters  $\sigma_{\Delta t_{1-i}}$  and  $\sigma_{d_{0-i}}$  can be calculated as the square root of the variance of the difference in TOA of the extensional mode to the sensors and square root of the variance of the distance from the sensor to the source. These variances can be estimated theoretically based on the error on identifying the time of arrivals as proposed by Niri and Salamone (2012) or statistically as proposed by Schumacher and Straub et al (2012). In here the parameters  $\sigma_{\Delta t_{1-i}}$  and  $\sigma_{d_{0-i}}$  are estimated statistically based on the probability distributions obtained by performing the same measure many times.

In this context the Bayes' theorem can be written as

$$p(\Theta|D, \mathcal{M}) \propto p(D|\Theta, \mathcal{M}) p(\Theta|\mathcal{M}) \quad (16)$$

where  $p(\Theta | D, M)$  represents the Probability Density Function (PDF) of  $\Theta$  for the chosen model  $M$  after being updated with the observation  $D$ , or posterior PDF,  $p(\Theta | M)$  is the PDF of the parameters  $\Theta$  for the chosen model  $M$  before updating, or prior PDF, and  $p(D | \Theta, M)$  is the likelihood of occurrence of the measurement  $D$  given the vector of parameters  $\Theta$  and the model  $M$ . The prior PDF is a mathematical representation of the engineering judgment on the unknown variables with the purpose of including any available knowledge prior to the experimental observations. For instance, in source locations algorithms the wave velocity in the medium is known with a good degree of confidence, then a Gaussian distribution with a small variance can be used to model the uncertainty on the wave velocity based on the prior knowledge.

Notice that Likelihood probability distribution is expressed differently for the MAE location methodology in which only the extensional mode is used Eq. (12) and the location methodology that uses both extensional and flexural modes Eq. (15). Assuming the uncertainty in the velocity of the extensional mode follows a Gaussian distribution, and then the no-normalized posterior PDF for the first MAE location methodology can be expressed as

$$p(\theta|D, \mathcal{M}) \propto \prod_{i=1}^n \exp\left(-\frac{1}{2}\left(\frac{\Delta t_i^{data} - \Delta t(\Theta)_i^{num}}{\sigma_{\Delta t_{1-i}}}\right)^2\right) \exp\left(-\frac{1}{2}\left(\frac{v_e^{theoretical} - v_e}{\sigma_{v_e}}\right)^2\right) \quad (17)$$

where  $v_e^{theoretical}$  is the theoretical extensional wave velocity and  $v_e$  is the extensional wave velocity used in the model. On the other hand for the second MAE methodology that uses both extensional and flexural modes the posterior PDF is expressed as

$$p(\theta|D, \mathcal{M}) \propto \prod_{i=1}^n \exp\left(-\frac{1}{2}\left(\frac{d_{0-i}^{data} - d_{0-i}(\Theta)^{num}}{\sigma_{d_{0-i}}}\right)^2\right) \exp\left(-\frac{1}{2}\left(\frac{v_e^{theoretical} - v_e}{\sigma_{v_e}}\right)^2\right) \exp\left(-\frac{1}{2}\left(\frac{v_f^{theoretical} - v_f}{\sigma_{v_f}}\right)^2\right) \quad (18)$$

where  $v_f^{theoretical}$  is the theoretical flexural wave velocity and  $v_f$  is the flexural wave velocity used in the model.

The parameters  $\Theta$  to update correspond to the unknown variables:  $x_0$  and  $y_0$  which represent the location of the source; and the wave velocities,  $v_e$  and  $v_f$ . Notice that the posterior PDF of Eq. (17) and Eq. (18) are a multivariable PDF of three and two dimensions respectively. The marginal distribution is calculated by sampling data from Eq. (17) and Eq. (18) through a Markov Chain Monte Carlo (MCMC) specifically the Metropolis-Hastings algorithm.

## Sampling

Sampling is used to obtain a set of samples from a larger set or population. Samples can be obtained from a PDF such as posterior distribution or from a set of data (resampling). In the case that the samples are obtained from a PDF, methods such as Markov Chain Monte Carlo (MCMC) and in specific the Metropolis-Hastings algorithm can be used. The algorithm is described in the following.

The Metropolis-Hastings algorithm generates a Markov chain where the proposed  $\Theta^{t+1}$  depends on the previous  $\Theta^t$ . Each candidate  $\Theta^{t+1}$  is generated by the density  $q(\Theta^{t+1}, \Theta^t)$  and the probability of moving from  $\Theta^t$  to  $\Theta^{t+1}$  is given by

$$\lambda(\theta^t, \theta^{t+1}) = \min\left\{\frac{p(\theta^{t+1}|D, \mathcal{M}) q(\theta^t, \theta^{t+1})}{p(\theta^t|D, \mathcal{M}) q(\theta^t, \theta^{t+1})}, 1\right\} \quad (19)$$

if  $p(\Theta^t | D, M) q(\Theta^t, \Theta^{t+1}) > 0$ , otherwise 1. Notice that  $p(\Theta | D, M)$  is present in the numerator and denominator. Therefore, the normalization constant of the joint distribution  $p(\Theta | D, M)$  does not have to be determined. The density function  $q(\Theta^{t+1}, \Theta^t)$  is chosen as  $q(\Theta^{t+1} - \Theta^t)$ , where  $q_1(\cdot)$  is a multivariable normal distribution. This results in the random walk  $\Theta^{t+1} = \Theta^t + z$ , where  $z$  is random and follows  $q_1(\cdot)$ . More information about the Metropolis-Hastings algorithm can be found in (Chib and Greenberg 1995, Robert and Casella 2004). The algorithm is run several times using different starting points and a number of initial samples are discarded. The sampling algorithm is run until convergence is reached based on Gelman, Carlin et al. (2004) criteria.

### Experimental Validation

This section presents the experimental validation of the Bayesian source location framework using PLBs on an aluminum plate  $\frac{1}{8}$ in thick and 36in by 36in. Four ultrasonic sensors  $\frac{1}{2}$ -2.25 manufactured by Xactex were used to capture the AE signals as shown in Figure 1. The signals were conditioned using  $\frac{3}{4}$ /6 preamplifiers at 40 dB, and then were acquired using a PCI2 system manufactured by Mistras Group. The waveforms were sampled at 10MHz and had a duration of 409.6 $\mu$ sec. Filters were set to let pass frequencies between 20KHz and 3MHz. PLBs were performed in three different locations as shown in Figure 2 and were repeated 40 times per location, for a total of 120 PLBs considering all locations.

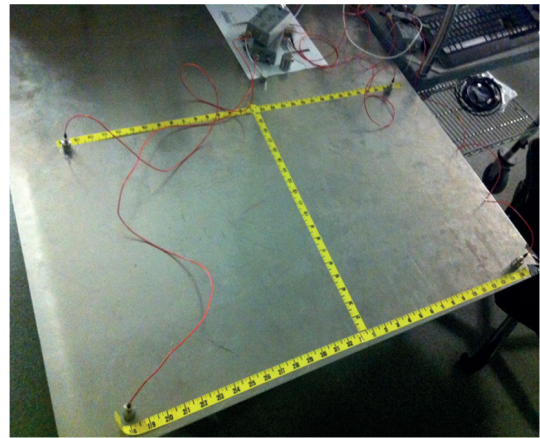


Figure 1. Aluminum plate used for PLBs location

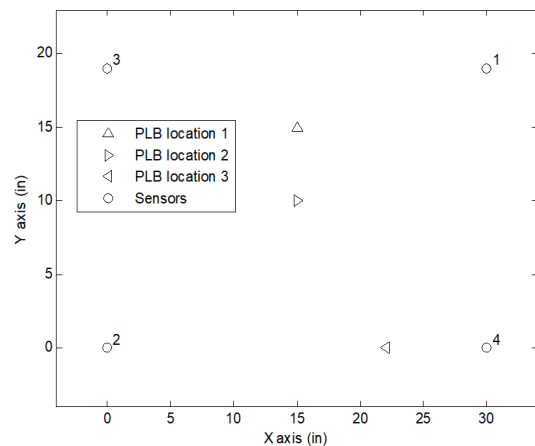


Figure 2. Sensors and PLBs locations

### Results

The reassigned scalograms were calculated for all waveforms captured from all PLB positions. The theoretical extensional (S0) and flexural (A0) modes were plotted as well, to match the reassigned scalogram using the non-dispersive points of the modes. Figure 3 shows typical reassigned scalograms from waveforms obtained in PLB position 1. The time of the arrival for each mode was identified by reading from the reassigned scalogram the TOA of the non-dispersive package that matches the specific mode.

The TOA of the extensional and flexural mode obtained from all 120 PLBs performed in the three PLBs positions shown in Figure 2. Figure 4 shows the histogram of the TOA of the extensional mode

for all sensors for PLB position 1. Figure 5 shows the histogram of the distance from the sensors to the source calculated for PLB position 1. Table I shows the variance of the TOA of the extensional mode for all sensors in all PLBs positions and Table II presents the variance of the distance between the sensors and the source for all PLBs positions. Notice that the variances in Table II and the histograms in Figure 5 are the result of the statistical representation of the TOA of the extensional mode, the flexural mode and the velocities of the extensional and flexural modes as shown in Eq. (13).

The location of the AE events were calculated for all PLB positions using the Bayesian inference framework proposed in here and the posterior distributions of Eq. (17) and Eq. (18) were sampled using the MCMC method. Figure 6 and Figure 7 show the calculated location of the AE event for PLB location 1 using the MAE methods 1 and 2 respectively. Figure 8 and Figure 9 show the computed location of the AE event for the PLB 2 using the MAE location methods 1 and 2 respectively. Figure 10 and Figure 11 show the calculated location of the AE event correspondent to PLB location 3 using the MAE location methods 1 and 2 respectively. Notice that in all PLB locations both methods MAE 1 and 2 locate the AE events to a region that encloses the actual PLB location. Additionally, notice that the MAE location method 2 has a noticeable larger region than MAE location method 1. This can be explained by the fact that MAE location method 2 depends on the TOA of both modes extensional and flexural, while the MAE location method 1 depends only on the TOA of the extensional mode. Identifying the TOA of both extensional and flexural modes is challenging. Notice that in most cases is easier to identify the TOA of the extensional mode because correspond to the portion of the wave that first arrive to the spectrogram. However, the extensional mode may disappear completely because of attenuation and may be confused with the flexural mode. On the other hand the flexural mode may be confused with reflections of the extensional mode. Thus identifying the TOA

of the flexural mode is more difficult than the extensional mode. Because MAE location method 2 uses both extensional and flexural mode, it is expected to have a larger uncertainty.

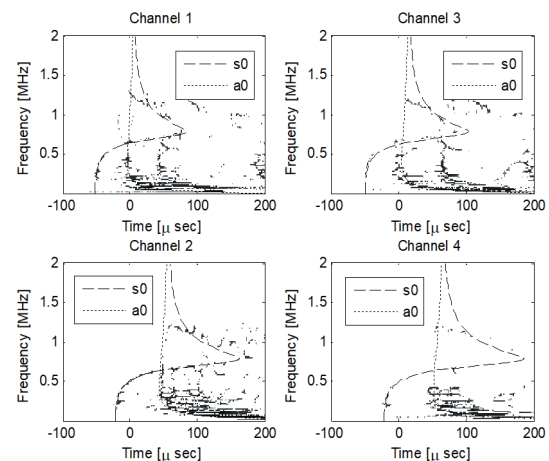


Figure 3. Typical reassigned scalograms for PLB position 1

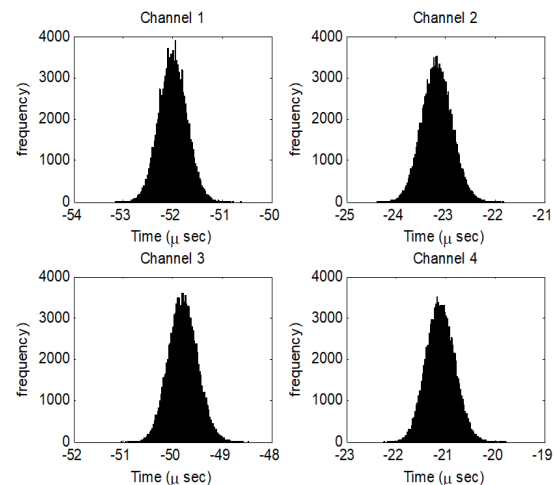


Figure 4. Distributions time of arrival extensional mode PLB position 1

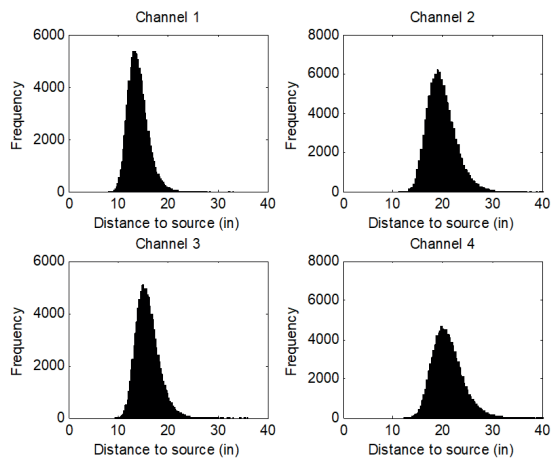


Figure 5. Distributions of time of arrival flexural mode PLB position 1

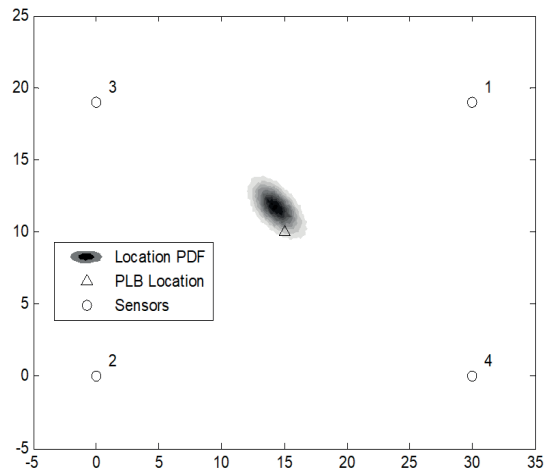


Figure 8. Marginal distribution source location using MAE method 1 PLB position 2

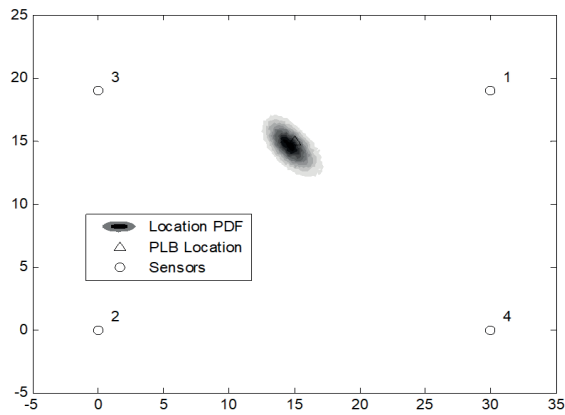


Figure 6. Marginal distribution source location using MAE method 1 PLB position 1

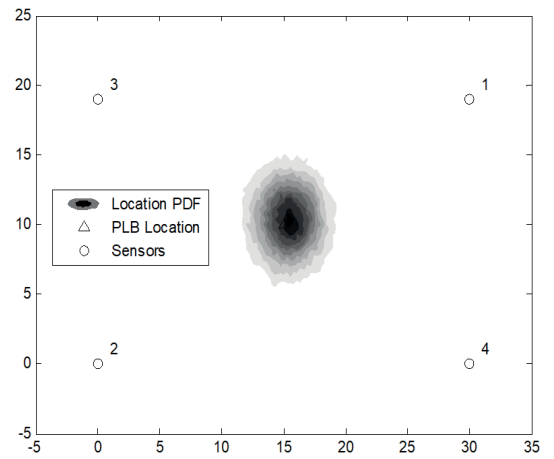


Figure 9. Marginal distribution source location using MAE method 2 PLB position 2

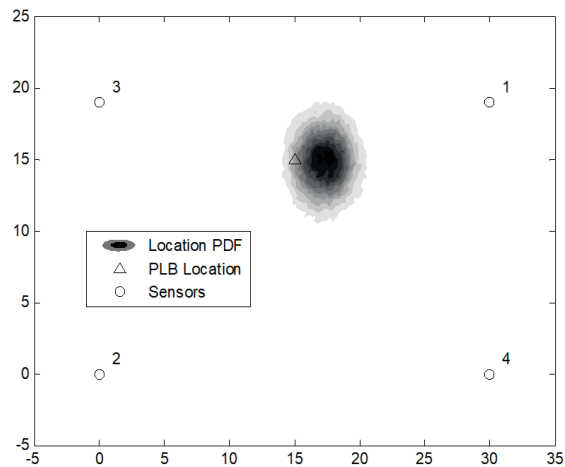


Figure 7. Marginal distribution source location using MAE method 2 PLB position 1

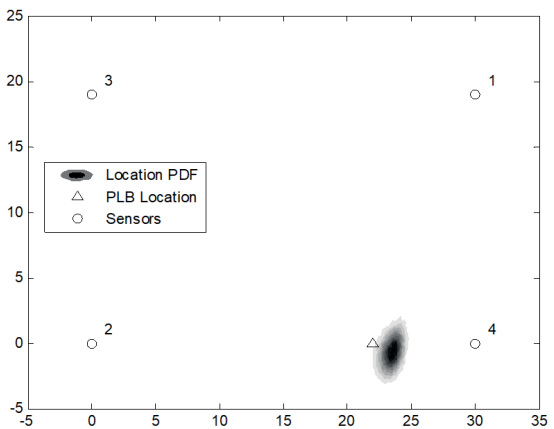


Figure 10. Marginal distribution source location using MAE method 1 PLB position 3

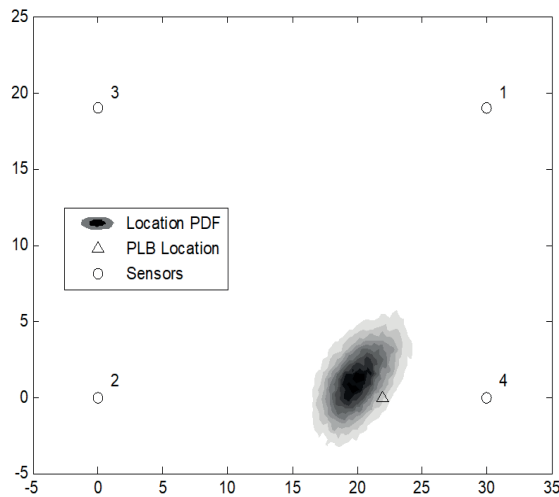


Figure 11. Marginal distribution source location using MAE method 2 PLB position 3

Table I. Calculated variance of the TOA extensional mode for all sensors and PLB positions

Channel	Variance ( $\mu\text{s}$ ) PLB 1	Variance ( $\mu\text{s}$ ) PLB 2	Variance ( $\mu\text{s}$ ) PLB 3
1	3.1	10.1	2.7
2	3.6	15.0	1.3
3	3.4	1.6	143.4
4	3.4	7.5	6.0

Table II. Calculated variance of the distance from the sensor to the source for all sensors and PLB positions

Channel	Variance (in) PLB 1	Variance (in) PLB 2	Variance (in) PLB 3
1	4.1	6.8	11.2
2	8.3	7.9	10.5
3	5.4	7.0	13.6
4	9.4	8.8	2.0

## Conclusions

This paper presents the uncertainty quantification of two MAE source location techniques. The first technique uses the TOA of only the extensional mode, and thus the source is located based on the difference in TOA of the extensional mode to the different sensors. The second MAE source location methodology uses the TOA of both the extensional and flexural modes, and then source is located based on the distance from the source to the sensors. Both

methodologies are implemented within a Bayesian framework.

The Bayesian framework was validated using an aluminum plate 36in by 36in and  $\frac{1}{8}$ in thick. A total of 120 PLBs were performed in three different locations in order to create a statistical representation of the TOA of the extensional and flexural modes. Then the posterior distribution of the MAE methods 1 and 2 was sampled using the Metropolis-Hastings algorithm.

In general it was more challenging to identify the TOA of the extensional mode in waveforms obtained far from source. Furthermore, in all sensors it was difficult to identify the TOA of the flexural mode because of reflections of the extensional mode. Results from the calculated probability of location of the PLBs for MAE methods 1 and 2 show that both methods can point to the correct region where the actual PLB was performed. However, MAE method 1 generates a noticeable smaller region than MAE method 2. This can be explained on the fact that MAE source location method 2 depends on both extensional and flexural TOA.

The increase in accuracy obtained with the re-assigned scalograms and the theoretical modes, as well as the known reliability obtained through Bayesian inference can lead to significant improvements in source location technology. In special the second MAE source location methodology that uses the time of arrival of both extensional and flexural modes have the potential to reduce significantly the number of sensors needed to monitor plate-like structures.

## References

- Aggelis, D.G., and Matikas, T.E. Effect of plate wave dispersion on the acoustic emission parameters in metals. *Comput. Struct.* 98–99 (2012) 17–22.
- Aki, K., and Richards, P. (2002), *Quantitative Seismology*, 2nd ed., W. H. Freeman and Company,

- San Francisco.
- Alleyne, D., and Cawley, P. (1991) A two-dimensional Fourier transform method for measurement of propagating multimode signals,” *J. Acoust. Soc. Am.*, 89, 1159–1168.
- Auger, F., and Flandrin, P. (1995). Improving the readability of time-frequency and time-scale representations by the reassignment method. *Signal Processing, IEEE Transactions on*, 43(5), 1068-1089.
- Scruby, C. (1987) An introduction to acoustic emission, *Journal of Physics E: Scientific Instruments* 20: 946-953.
- Bao, J. (2003) Lamb wave generation and detection with piezoelectric wafer active sensors. Ph.D. Thesis, College of Engineering and Information Technology, University of South Carolina
- Beck JL, Katafygiotis LS. Updating models and their uncertainties. I: Bayesian statistical framework. *J Eng Mech* 1998;124:455–61.
- Chib S, Greenberg E. Understanding the Metropolis–Hastings algorithm. *Am Statist* 1995;49:327–35.
- Cuadra, J., Vanniamparambil, P. A., Servansky, D., Bartoli, I., and Kontsos, A. (2015). Acoustic emission source modeling using a data-driven approach. *Journal of Sound and Vibration*.
- Eisenhardt, C., Jacobs, L., and Qu, J. (1999) Application of laser ultrasonics to develop dispersion curves for elastic plates, *J. Appl. Mech.*, 66, 1043–1045.
- Gelman, A., Carlin, J. B., Stern, H. S., and Rubin, D. B. (2004). *Posterior simulation Chapter 11, Bayesian data analysis*, CRC Press, Boca Raton, FL, 296–297. [1] ASCE. Report Card for America's Infrastructure. American Society of Civil Engineers (ASCE); 2009.
- Giurgiutiu, V. (2008) *Structural Health Monitoring with Piezoelectric Wafer Active Sensors: Academic Press (an Imprint of Elsevier)*
- Godinez-Azcuaga, V., Inman, D., Ziehl, P., Giurgiutiu, V., Nanni, A. (2011) Recent advances in the development of a self-powered wireless sensor network for structural health prognosis. In: Wu HF, editor. 1 ed. San Diego, California, USA: SPIE; p. 798325-7.
- Goodman, L. (1952) Circular-crested vibrations of an elastic solid bounded by two parallel planes, *Proc. 1st U. S. Nat. Congr. Appl. Mech.*
- Gorman, M. and Prosser, W. (1991) AE Source Orientation by Plate Wave Analysis, *Journal of Acoustic Emission*, Vol. 9(4), (1991) pp. 283-288.
- Goupillaud, P., Grossmann, A., and Morlet, J. (1984). Cycle-octave and related transforms in seismic signal analysis. *Geoexploration*, 23(1), 85-102.
- Graff, K. (1975) *Wave motion in elastic solids* (Ohio State University Press, Columbus)
- Grosamann, A. and Morlet, J. (1984) Decomposition of Hardy functions into square integrable wavelets of constant shape, *SIAM J. Math.*, vol. 15. pp. 723-736.
- Jaynes, E. (2003) *Probability Theory: The Logic of Science*. Cambridge University Press.
- Kennedy M, O’Hagan A. Bayesian calibration of computer models. *J Roy Statist Soc Ser B: Statist Methodol* 2001;63:425–64.
- Klaes, M. (1978) in *Journées d'Etudes sur l'Émission Acoustique*, INSA de Lyon (France)
- Nair, A. and C. S. Cai (2010). Acoustic emission monitoring of bridges: Review and case studies *Engineering Structures* 32(6): 1704-1714.
- Niethammer, M., Jacobs, L., Qu, J., and Jarzynski, J. (2000) Time-Frequency Representation of Lamb Waves Using the Reassigned Spectrogram, *J. Acoust. Soc. Am.*, 107, pp. L19–L24
- Niri ED, Salamone S. A probabilistic framework for acoustic emission source localization in plate-like structures. *Smart Materials and Structures*. 2012;21:035009.
- Ozevin, D., and Harding, J. (2012). Novel leak localization in pressurized pipeline networks using acoustic emission and geometric connectivity. *International Journal of Pressure Vessels and Piping*, 92, 63-69.
- O’Hagan, A., and Oakley, J. (2004). “Probability is perfect, but we can’t elicit it perfectly.” *Reliab. Eng. Syst. Saf.*, 85(1–3), 239–248.
- Robert CP, Casella G. Monte Carlo statistical me-

- thods 2nd ed.. Springer Verlag; 2004.
- Rose J L 1999 Ultrasonic Waves in Solid Media (Cambridge: Cambridge University Press).
- Schumacher, T., Straub, D., Higgins, C. (2012). Toward a probabilistic acoustic emission source location algorithm: A Bayesian approach. *Journal of Sound and Vibration*, Vol. 331(19), pp. 4233-4245.
- Shigeishi, M., S. Colombo, K. J. Broughton, H. Rutledge, A. J. Batchelor and M. C. Forde (2001). Acoustic emission to assess and monitor the integrity of bridges, *Construction and Building Materials* 15(1): 35-49.
- Teolis, A. (1998), *Computational signal processing with wavelets*, Birkhauser, pp. 65.
- Yan, Gang, and Jianfei Tang. (2013) "A Bayesian approach for acoustic emission source location in plate-like structure." Singapore International NDT Conference & Exhibition, 19-20 July 2013.
- Zárate, B. A., Caicedo, J. M., Yu, J., and Ziehl, P. (2012). Probabilistic Prognosis of Fatigue Crack Growth Using Acoustic Emission Data. *Journal of Engineering Mechanics*, 138(9). Chicago.
- Zárate, B. A., Pollock, A., Momeni, S., and Ley, O. (2015). Structural health monitoring of liquid-filled tanks: a Bayesian approach for location of acoustic emission sources. *Smart Materials and Structures*, 24(1), 015017.